Nanopatterned dual reactive surface-driven by block copolymer self-assembly

Coste Mawélé Loudy, Joachim Allouche, Antoine Bousquet, Hervé Martinez, Laurent Billon

Nanopatterned dual reactive surface-driven by block copolymer self-assembly

Coste Mawélé Loudy [1,2], Joachim Allouche [1], Antoine Bousquet [1], Hervé Martinez [1] Laurent Billon [1,2]**

[1] CNRS/Université de Pau et des Pays de l'Adour/E2S UPPA, IPREM CNRS-UMR 5254 Hélioparc, 2 avenue Président Angot, 64053 Pau Cedex 9, France

[2] Bio-inspired Materials Group: Functionality & Self-assembly, Université de Pau et des Pays de l'Adour, IPREM CNRS-UMR 5254, Hélioparc, 2 avenue Président Angot, 64053 Pau Cedex 9, France

Corresponding Authors:

Herve.martinez@univ-pau.fr

Laurent.billon@univ-pau.fr

ABSTRACT.

Herein, we report the functionalization of selective nano-domains driven by the self-assembly of a polystyrene-*block*-poly(vinyl benzyl azide) PS-*b*-$PVBN_3$ copolymer synthesized in three steps. First, a Polystyrene macro-initiator was synthesized, and then extended with vinyl benzyl chloride by Nitroxide Mediated Polymerization to form a polystyrene-*block*-poly(vinyl benzyl chloride) PS-*b*-PVBC. Nucleophilic substitution of the chloride into an azide moiety is then performed to obtain the PS-*b*-PVBN which self-assembled to form cylindrical domains of polystyrene and vinyl benzyl azide. Click chemistry was then used to chemically bind functional gold nanoparticles and poly(N-isopropylacrylamide) (PNIPAM) on $PVBN_3$ domains due to the specific anchor at the surface of the nanopatterned film. Atomic Force Microscopy (AFM) was used to observe the block copolymer self-assembly and gold nanoparticles alignment at the surface of the $PVBN_3$ nanodomains. Thorough X-ray Photoelectron Spectroscopy (XPS) analysis of the functional film showed the evidence of the sequential grafting of nanoparticles and PNIPAM. The hybrid surface expressed thermoresponsive properties and serve as pattern to perfectly align and control the assembly of inorganic particles at the nanoscale.

Keywords: thermoresponsive surface, patterned surface, click chemistry, gold nanoparticle, self-assembly, grafting

Introduction

The self-assembly of block copolymers (BCPs) at the nanoscale is attracting more and more research fields because of its various applications for emerging nanotechnologies such as sensors, organic optoelectronics, catalytic nanostamps, transistors and nanotemplating.[1] Among their various applications, the fabrication of patterned surfaces with a spatial resolution below 50 nm which cannot be reached by traditional lithographic means, has recently gained significant attention.[2,3] Moreover researchers have shown that BCP self-assembly could serve as a template for localized surface modification. Delaittre *et al.* have reported some examples of phase-segregating block copolymer systems to produce controlled nanopatterned platforms for further surface modification.[4,5] The authors synthesized derivatives of polystyrene-*block*-polyisoprene bearing reactive functions towards Huisgen cycloaddition, or nucleophilic substitution reactions to produce a surface-reactive nanostructured films with 30 nm domains. Billon *et al.* also reported the fabrication of a triple structured honeycomb film made with a polystyrene-*block*-poly(4-vinylbenzylchloride). The patterned surface was then modified by azidation and subsequent Huisgen cycloaddition with organic molecules to obtain a pH-triggered wettability.[6,7]

This reactive patterning technology is getting even more interest in biological systems and medicine where the precise localization and the proximity of some proteins and enzymes are required for efficiency.[8] For example, the interaction between the cell and the extracellular matrix (ECM) is done through transmembrane cell adhesion proteins responsible of the signal transduction.[11] The principal receptors on animal cells for binding most extracellular matrix are integrins. The linkage of ECM to the cell is done through some specific sites called focal adhesions (FAs), by which the cell can recognize biochemical features, process and explore external stimuli.[12] The spatial organization and the spacing of integrins are key factors for the succesful recognition of biological systems and stimuli. Usually spacing below 100 nm is required, and can be achieved through the grafting of the receptors on gold nanoparticle patterns, obtained through block copolymers self-assembly. Arnold and co-workers proposed that the range between 58-73 nm was a universal ligand spacing for integrins.[13–15] They used polystyrene-*block*-poly(2-vinylpyridine) (PS-*b*-P2VP) micelle nanolithography to prepare surface patterned with gold nanodot of 8 nm diameters. This platform provided precise anchor

point for integrin molecules that reacted through the cysteine groups of their beta subunits. Using the self-assembly of various compositions of PS-*b*-P2VP, they were able to design the space between the gold mono-anchors from 28 nm to 85 nm.[13]

Stimuli responsive surfaces are getting more and more attractive due to their ability to change their physical properties when subjected to different stimuli as temperature, light or pH. Such surfaces can offer many applications in medicine[16,17], bacterial biofilm[19], tissue engineering[20] , cell culture[21] , mammalian cell release surfaces[22] and controlled delivery.[23] Since the first work of Heskins and *al.*[24] who showed that bulk poly(N-isopropylacrylamide) (PNIPAM) could express a lower critical solution temperature (LCST) close to the physiological temperature (32° C in water), many works have been done to investigate the thermoresponsive properties of surfaces modified by poly(N-isopropylacrylamide) (PNIPAM).[25,26] The aim of all those methods is to induce a switch of the surface wettability, from hydrophilic to hydrophobic when the temperature is increased above the LCST. When grafted onto the surfaces of cell culture dishes, PNIPAM can exhibit this behaviour allowing the proliferation and attachment of biological cells around 37° C (physiological temperature) and their removal from the surface around 20° C.[31]

In this work we report the functionalisation of selective domains of a nanopatterned polymer thin film made of polystyrene-*block*-poly(4-vinylbenzyl azide) (PS-*b*-$PVBN_3$). The polymer self-assembled into *in-plane* cylinders of poly(4-vinylbenzyl azide) that can be post-modified *via* Huisgen cycloaddition with both organic and inorganic materials, without modifying the surface structuration. Ethynyl-terminated PNIPAM and propargyl-capped-gold nanoparticles were covalently grafted to the surface of the film through click reaction with the azide group of the $PVBN_3$ block (Scheme 1). The functionalized surface shows reversible thermoresponsive properties due to the presence of PNIPAM. Moreover, the spatial organization of gold nanoparticles patterned by the block copolymer self-assembly and separated by thermoswitchable PNIPAM could be a good candidate for single anchor points template for biochemical systems, as mentioned by Arnold *et al.*, previously.[19-21]

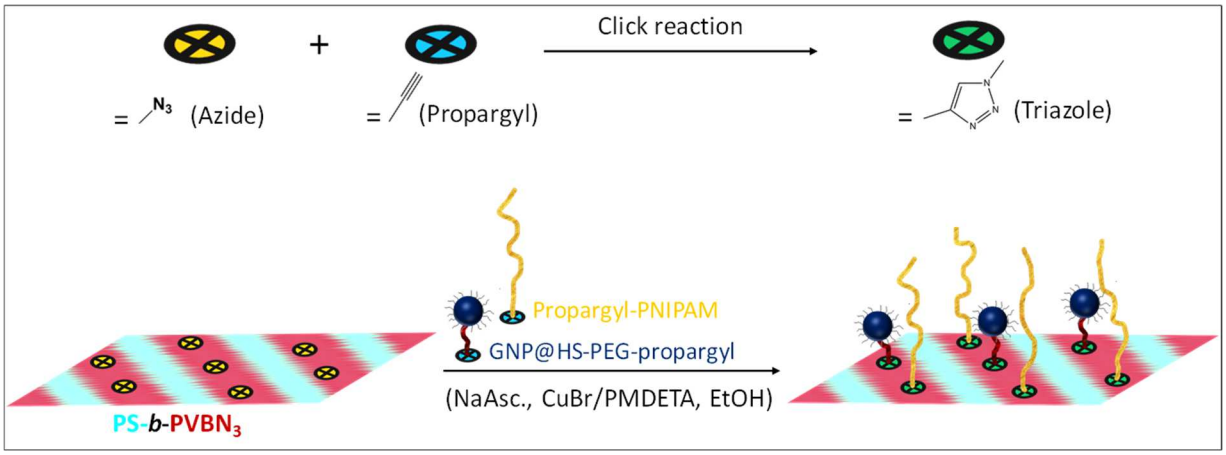

Scheme 1. Synthetic pathway for the dual grafting of PNIPAM and gold nanoparticles onto $PVBN_3$ domains of a nanopatterned film of PS-*b*-$PVBN_3$.

Results and Discussion

The polystyrene-*block*-poly(4-vinylbenzylazide) (PS-*b*-$PVBN_3$) was synthesized in three steps *via* radical polymerization and nucleophilic substitution reaction (scheme SI1). Styrene was first polymerized by NMP using Blockbuilder® as initiator and controlling agent. The reaction was stopped at 50% conversion (followed by ^{1}H NMR) to ensure a high fraction of nitroxide end-functional chains. After purification the PS macro-initiator was used to polymerize 4-vinylbenzylchloride (VBC) to form PS-*b*-PVBC which, after reaction with NaN_3, led to the formation of the final block copolymer (PS-*b*-$PVBN_3$). ^{1}H NMR analysis have been carried out to determine the molar composition of the final block copolymer as PS_{330}-*b*-$(PVBN_3)_{150}$ (see supporting information Figure SI1 and Table SI1). The size exclusion chromatograms of both the macro-initiator (PS-SG1) and the final block copolymer (PS-*b*-$PVBN_3$) in THF are reported in supporting information (Figure SI2). A narrow dispersity was observed for PS ($Đ$ = 1.1) and PS-*b*-$PVBN_3$ ($Đ$ = 1.2) as reported in literature for PS and derivatives synthesized by Nitroxide-Mediated Polymerization.[6,32] The molar mass of PS-*b*-$PVBN_3$ calculated from SEC analysis using PS calibration was found to be equal to 49 000 g.mol^{-1}.

The elaboration of a hybrid functional surface from self-assembled films of PS-*b*-$PVBN_3$ studied in this work was done through a chemical grafting *via* Huisgen cycloaddition between azide groups at the surface of PS-*b*-$PVBN_3$ film and alkyne functionalized materials. For this reason, propargyl-terminated PNIPAM was synthesized by ATRP using propargyl 2-bromoisobutyrate, an ATRP initiator with a carbon-carbon triple bond. For the same purpose, 5 nm gold nanoparticles were prepared in one step using a poly(ethyleneglycol) (PEG) ligand

bearing a propargyl group and $HAuCl_4.6H_2O$ salt. Details about the synthesis and characterization of those two materials can be found in supporting information (Figures SI3-8, Tables SI2-3).

Films were prepared through the drop-casting of a PS-*b*-PVBN3 solution in chloroform (10 $g.L^{-}1$) on a glass slide. It is well known that linear diblock copolymer self-assembly depends on three parameters as predicted by the self-consistent mean-field theory: the volume fraction of the blocks (*f*), the total degree of polymerization (*N)* and the interaction between the two segments (χ, Fluory-Huggins parameter)[33]. Using the degree of polymerisation of the blocks (330 for styrene and 150 vinylbenzyl azide), the volume fraction of PS has been calculated and was equal to 0.63, characteristic value for a thermodynamic assembly into hexagonal-close-packed (*hcp*) cylinders. AFM images of the top surface of PS-*b*-$PVBN_3$ film are depicted in Figure 1a. Parallel cylinders of $PVBN_3$ (red colour) in a PS matrix (green colour) can clearly be observed. Such a structuration is in agreement with the previous calculated volume fractions and with PS-based block copolymers reported in the literature with similar composition.[33–36] It is worth noting that no thermal or solvent annealing were performed to reach the thermodynamic equilibrium of the hcp feature. From this image, we could also observe that PS has a higher adhesion value than $PVBN_3$. After the click reaction with the alkyne modified particles, the AFM images showed black dots with a low adhesion value pertaining to the gold nanoparticles grafted at the top surface of the copolymer film (Figure 1b). It is clear that the nanoparticles are only grafted on the $PVBN_3$ domains of the nanopatterned surface bearing the reactive azide anchor. When alkyne-functionalized PNIPAM was grafted onto $PVBN_3$ domains (Figure 1c and 1d), a significant shift of the adhesion value was observed (from 17.2 mV to 69 mV), indicating the successful anchoring of PNIPAM.

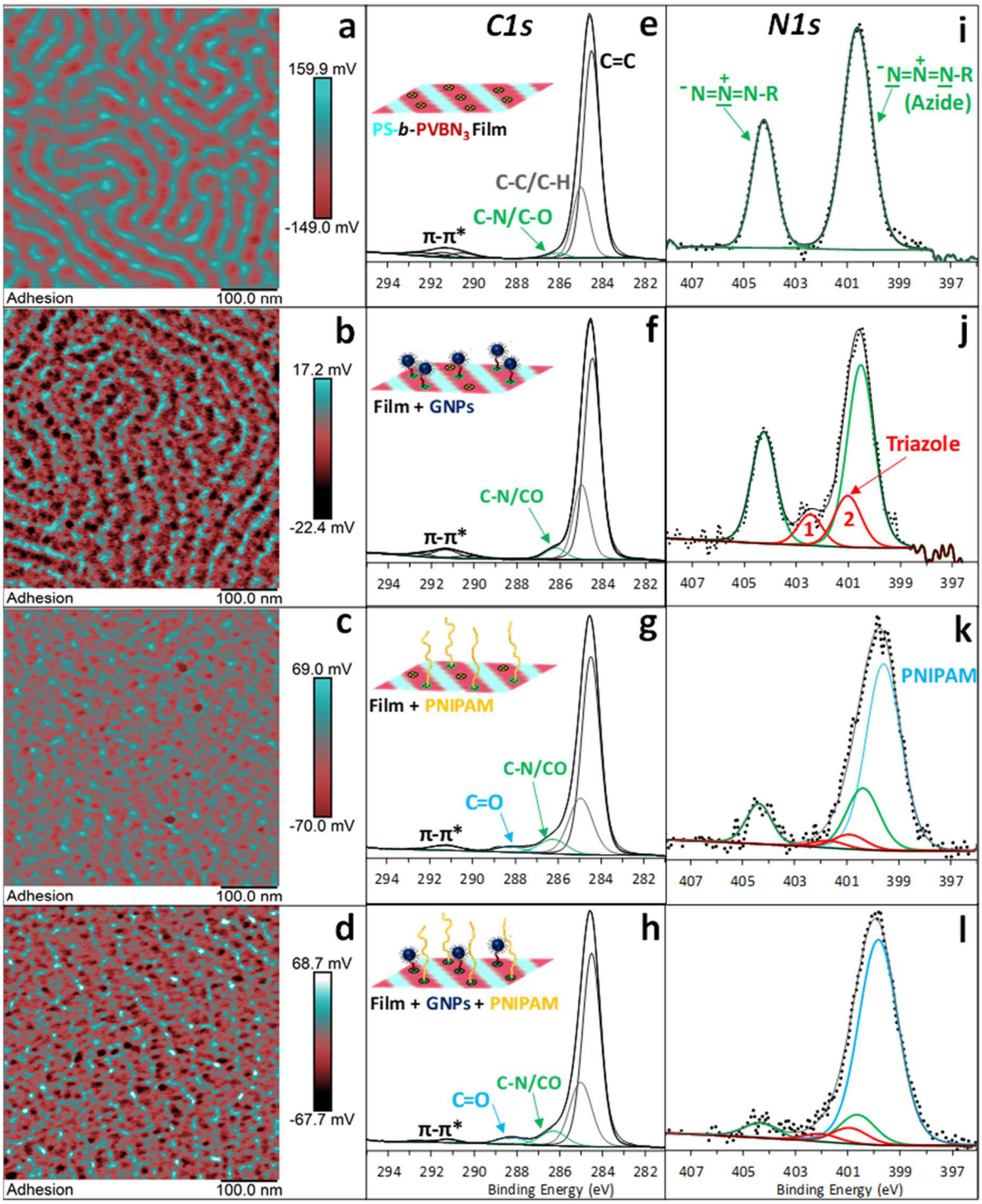

Figure 1. AFM images, C 1s and N 1s spectra from XPS analysis of bare PS-*b*-PVBN$_3$ film (a,e,i) and PS-*b*-PVBN$_3$ film grafted with: GNPs (b,f,j), PNIPAM (c,g,k) and both GNP and PNIPAM (d,h,l).

X-ray photoelectron spectroscopy (XPS) was performed on the different films: PS-*b*-PVBN$_3$, PS-*b*-PVBN$_3$ grafted with both gold nanoparticles and PNIPAM and PS-*b*-PVBN$_3$ grafted with each separate materials. Note that XPS experiments were carried out at nitrogen temperature to avoid degradation effects under the X-ray beam. The C 1s spectrum (Figure 1e)

of PS-*b*-PVBN$_3$ film presented 4 components: C=C from aromatic rings (sp2, 284.5 eV), C−C/C−H from vinylic bonds (sp3, 285 eV) that could also include aliphatic carbon from contamination, C-N from PVBN$_3$ block. (286.2 eV) and π-π* transition component around 291 eV (Figure 1e). N 1s high resolution spectrum is depicted in Figure 1i. The characteristic azide spectrum was best fitted with 2 components (intensity ratio 1:2, in agreement with the chemical formula of azide): the positively charged nitrogen (404.2 eV) and the neutral and negatively charged nitrogen peak (400.5 eV)[37]. The total contribution of nitrogen represented 1.8 % in atomic percentage (Table SI4). The success grafting of gold nanoparticles at the surface of PS-*b*-PVBN$_3$ can clearly be observed from both carbon and nitrogen spectra (Figure 1f, 1j). Indeed, an increase of the intensity of the component at 286.2 eV is observed, due to C−O and C−S bonds from PEG-propargyl ligand at the surface of gold nanoparticles. Note that C−O, C−N and C−S have the same binding energy range and cannot be discriminated. A detailed quantification (Table SI5) from N 1s, O 1s and S 2p high resolution spectra showed that more than half of the intensity of that peak (2.8/4.1) comes from C−O and C−S bonds. The atomic percentage of nitrogen (azide peaks) slightly decreased (1.5 %) compared to PS-*b*-PVBN$_3$ sample (1.8 %). Moreover, a new component is observed under the same area at 401 eV (labelled 2, figure 1j) with an intensity that is twice the one of the arising peak around 402.5 eV (labelled 1, figure 1j), in agreement with triazole binding energy as reported in literature.[38–41] The triazole environment (0.4 at. %) is only a fraction of the total amount of nitrogen detected by XPS (1.9 at. %), meaning that only 21% of the azide-anchors present at the surface of the film reacted with the ligands of gold nanoparticles. This quantitative XPS information is in line with the AFM observation where we can clearly observe black dots of gold nanoparticles between which the polymer is still visible. Thus the remaining azide-anchors can been used for further functionalization of the surface with PNIPAM polymer to create a thermoresponsive surface. Prior to this, PNIPAM was grafted on bare PS-*b*-PVBN$_3$ film. Figure 1c shows the AFM image of the surface where the nanophase segregation is still visible. XPS was also used to confirm the anchoring of PNIPAM with the increase of C−N component at 286.2 compared to PS-b-PVBN$_3$ sample (Figure 1k and 1e). Moreover, a new component attributed to C=O can be observed, in agreement with the chemical formula of PNIPAM. The XPS N core peak (Figure 1k) presents a component located at 399 eV attributed to the secondary amide environment of PNIPAM.

The successful grafting of PNIPAM on PS-*b*-PVBN$_3$ films modified with gold nanoparticles was finally proved by XPS with changes occurring on C 1s and N 1s spectra of

the sample (Figure 1h, 1l). First, an increase of C–N component at 286.4 eV (5.6 %) is noticeable compared with the sample of the film grafted with nanoparticles (4.0 %). Secondly, the apparition of C=O bond (288.3 eV) from the acrylamide group can be observed. The decrease of the intensity of the shake-up transition (291 eV) agrees with the addition of non-aromatic organic compound. The total amount of nitrogen increased from 1.9 % before grafting PNIPAM (Table SI5) to 2.9 % after reaction (Table 1). The intensity of azide positively charged peak at 404.2 eV decreased and triazole relative compounds (400.9 and 402 eV) increased due to the click reaction. Eventually, a strong intensity peak was observed at 399.9 eV, characteristic of nitrogen environment in PNIPAM[42].

Table 1. XPS data of the final hybrid film after the dual grafting of GNPs@propargyl-PEG4-thiol and propargyl-PNIPAM on PS-*b*-PVBN$_3$ film.

Orbitals	Components	BE (eV)	FWHM (eV)	At. Conc. (%)
Au 4f	$4f_{7/2-5/2}$	84.0–88.8	1.1–1.2	0.2
C 1s	C=C (cycle)	284.5	1.0	57.6
	C–C/C–H	285.0	1.4	23.6
	C–N/C–O	286.4	1.4	5.6
	O=C	288.3	1.4	3.0
	π-π*	291.2	1.0	1.5
N 1s	N_{PNIPAM}	399.9	1.8	2.2
	Azide	400.5–404.3	1.6–1.6	0.45
	Triazole	400.9–402.5	1.8–1.6	0.25
O 1s	O=C	531.7	1.8	3.7
	O–C	532.8	1.8	2.3

The wettability of the surfaces was studied using water contact angle measurements. No significant changes were observed for the contact angle value of PS-*b*-PVBN$_3$ films before (92°) and after (90°) grafting gold nanoparticles (Figure SI9). Pure PNIPAM films, however, exhibited remarkable change of the water contact angle (CA) with temperature. As expected, at 25°C the CA was 31° whereas at 45°C it raised to 65° with a persistent reversible behaviour during at least 4 cycles, as shown in Figure 2. It is well known thast below its lower critical solution temperature (LCST, 32 °C), PNIPAM polymer chains are swollen, due to high interactions by hydrogen bonds with water that makes the polymer hydrophylic.[43,44] When the temperature is beyond its LCST, the hydrogen bonds weaken and the chains collapse into a hydrophobic state by water release. Finally, PNIPAM chains grafted specifically on PBVN$_3$ domains exhibited the same thermoresponsive behaviour, with water angle contact switching

from 78° at room temperature (25 °C) to 92° when heated at 45 °C (Figure 2). This amplitude, weaker than for the pure PNIPAM film, is in agreement with the surface fraction (40%) of the PS-*b*-PVBN$_3$ film effectively grafted with PNIPAM.

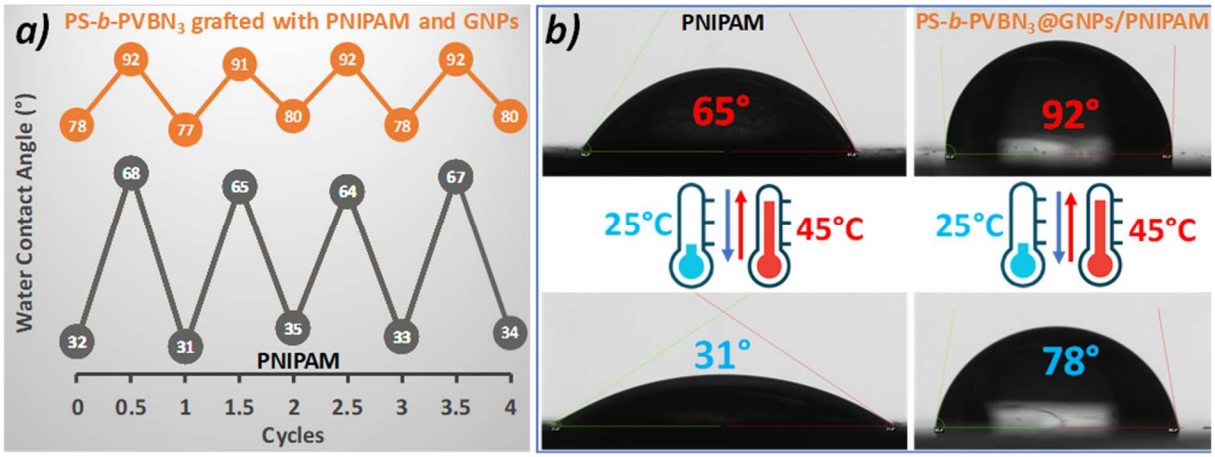

Figure 2. (a) Reversible wettability behaviour of pure PNIPAM film (grey) and PS-*b*-PVBN$_3$ film grafted with PNIPAM (orange), observed through the measurement of water contact angle at 25 and 45 °C. (b) Pictures of the corresponding water droplets.

Conclusion

PS-*b*-PVBN$_3$ diblock copolymer is an excellent material to produce functional nanopatterned surfaces. PS$_{330}$-*b*-(PVBN$_3$)$_{150}$ self-assembles into well distinct cylinders of PVBN$_3$ into a PS matrix. The azide groups at the surface of the PVBN$_3$ domains are accessible and can serve as anchors to chemically bind both organic compounds and inorganic nanoparticles. A precise surface analysis by XPS, carried out under rigorous conditions like negative temperature, appeared to be a good tool to monitor quantitatively the reaction of likely unstable organic functions such as azide groups. The block copolymer surface grafted with PNIPAM exhibits thermoresponsive properties with significant changes of the contact angle at room temperature and above the LCST. Moreover, the grafting of PNIPAM in the inter-particle space to produce thermo-responsive surfaces can be a tool to trigger the cell adhesion. This property, combined with the chemical attachment of gold nanoparticles could offer a nanopatterned template for functionalization with integrins, allowing efficient interaction with living system through the so-called focal adhesion.

Experimental section

Materials Synthesis: See Synthesis section in the supporting information.

Chemicals, reagents: Propargyl-PEG4-thiol (90%) was brought from Brodpharm (USA). All other chemicals were purchased from Sigma Aldrich and used without further purification except copper bromide (CuBr) which was purified by stirring with acetic acid overnight, washing with acetic acid, absolute ethanol and diethyl ether before finally be dried in a vacuum oven.

Preparation of the hybrid film: Films were prepared through a drop-casting process. A 10 $g.L^{-1}$ solution of PS-*b*-$PVBN_3$ in chloroform was carefully drop-casted on a microscope glass slide to form a continuous film after the evaporation of the solvent. This led to a well-organized structure with distinct domains of PS and $PVBN_3$ on which selective click reactions were performed were performed on the extreme surface of PS-*b*-$PVBN_3$, allowing therefore to chemically bind successively both inorganic nanoparticles PNIPAM. Propargyl-PEG4-thiol-capped gold nanoparticles were first clicked on $PVBN_3$ nanodomains. CuBr (4 mg), sodium ascorbate (4 mg) and PMDETA (5 mL) were added to a plastic tube containing 10 mL of ethanol. The mixture was stirred before adding 5 mL of the synthesized suspension of gold nanoparticles. Finally, the microscope slide containing the self-assembled film was dipped into the mixture for overnight. Then the glass was vigorously washed in ethanol several times and whether dried before the click reaction with Ethynyl terminated PNIPAM using the same procedure.

Characterization: ^1H NMR experiments were carried out on a Bruker 400 MHz spectrometer in CDCl3 at 27 °C. XPS measurements were performed using an Escalab 250 Xi spectrometer using a monochromatized Al Kα radiation (hν = 1486.6 eV) at liquid nitrogen temperature. Atomic force microscopic (AFM) images were obtained using MultiMode® 8 Atomic Force Microscope (AFM) from Bruker in a PeakForce QNM (Quantitative NanoMechanics) mode. Transmission Electron Microscopy images of gold nanoparticles were performed on a Philips CM 200 (200 kV) TEM microscope equipped with a LaB6 source. Contact Angle measurements were done using an instrument designed in the Lab. The apparatus was made of an optical bench equipped with a heat control unit that can reach till 200 °C, a humidity control system and an ethernet camera that can record 30 images per second. Angle angles were obtained through the analysis of the images using LabVIEW software.

References:

[1] H.-C. Kim, S.-M. Park, W. D. Hinsberg, *Chem. Rev.* **2010**, *110*, 146.

[2] S. Park, D. H. Lee, J. Xu, B. Kim, S. W. Hong, U. Jeong, T. Xu, T. P. Russell, *Science* **2009**, *323*, 1030.
[3] H. S. Suh, D. H. Kim, P. Moni, S. Xiong, L. E. Ocola, N. J. Zaluzec, K. K. Gleason, P. F. Nealey, *Nat. Nanotechnol.* **2017**, *12*, 575.
[4] H. Turgut, N. Dingenouts, V. Trouillet, P. Krolla-Sidenstein, H. Gliemann, G. Delaittre, *Polym. Chem.* **2019**, *10*, 1344.
[5] D. Varadharajan, H. Turgut, J. Lahann, H. Yabu, G. Delaittre, *Adv. Funct. Mater.* **2018**, *28*, 1800846.
[6] P. Marcasuzaa, S. Pearson, K. Bosson, L. Pessoni, J.-C. Dupin, L. Billon, *Chem. Commun.* **2018**, *54*, 13068.
[7] P. Marcasuzaa, H. Yin, Y. Feng, L. Billon, *Polym. Chem.* **2019**, *10*, 3751.
[8] S. Schoffelen, J. C. M. van Hest, *Soft Matter* **2012**, *8*, 1736.
[9] F. Xia, L. Feng, S. Wang, T. Sun, W. Song, W. Jiang, L. Jiang, *Adv. Mater.* **2006**, *18*, 432.
[10] J. Lindqvist, D. Nyström, E. Östmark, P. Antoni, A. Carlmark, M. Johansson, A. Hult, E. Malmström, *Biomacromolecules* **2008**, *9*, 2139.
[11] R. O. Hynes, *Cell* **1992**, *69*, 11.
[12] B. Geiger, A. Bershadsky, R. Pankov, K. M. Yamada, *Nat. Rev. Mol. Cell Biol.* **2001**, *2*, 793.
[13] M. Arnold, E. A. Cavalcanti-Adam, R. Glass, J. Blümmel, W. Eck, M. Kantlehner, H. Kessler, J. P. Spatz, *ChemPhysChem* **2004**, *5*, 383.
[14] E. A. Cavalcanti-Adam, A. Micoulet, J. Blümmel, J. Auernheimer, H. Kessler, J. P. Spatz, *Eur. J. Cell Biol.* **2006**, *85*, 219.
[15] C. Selhuber-Unkel, T. Erdmann, M. López-García, H. Kessler, U. S. Schwarz, J. P. Spatz, *Biophys. J.* **2010**, *98*, 543.
[16] G. Zhou, L. Veron, A. Elaissari, T. Delair, C. Pichot, *Polym. Int.* **2004**, *53*, 603.
[17] D. Duracher, A. Elaïssari, F. Mallet, C. Pichot, *Langmuir* **2000**, *16*, 9002.
[18] H. Kanazawa, Y. Kashiwase, K. Yamamoto, Y. Matsushima, A. Kikuchi, Y. Sakurai, T. Okano, *Anal. Chem.* **1997**, *69*, 823.
[19] D. Cunliffe, C. de las Heras Alarcón, V. Peters, J. R. Smith, C. Alexander, *Langmuir* **2003**, *19*, 2888.
[20] L.-S. Wang, P.-Y. Chow, T.-T. Phan, I. J. Lim, Y.-Y. Yang, *Adv. Funct. Mater.* **2006**, *16*, 1171.
[21] B. Voit, D. Schmaljohann, S. Gramm, M. Nitschke, C. Werner, *Int. J. Mater. Res.* **2007**, *98*, 646.
[22] Y. Ito, G. Chen, Y. Guan, Y. Imanishi, *Langmuir* **1997**, *13*, 2756.
[23] S. Dinçer, A. Tuncel, E. Pişkin, *Macromol. Chem. Phys.* **2002**, *203*, 1460.
[24] M. Heskins, J. E. Guillet, *J. Macromol. Sci. Part - Chem.* **1968**, *2*, 1441.
[25] V. P. Gilcreest, W. M. Carroll, Y. A. Rochev, I. Blute, K. A. Dawson, A. V. Gorelov, *Langmuir* **2004**, *20*, 10138.
[26] F. Montagne, J. Polesel-Maris, R. Pugin, H. Heinzelmann, *Langmuir* **2009**, *25*, 983.
[27] J. N. Kizhakkedathu, R. Norris-Jones, D. E. Brooks, *Macromolecules* **2004**, *37*, 734.
[28] C. Bo, Y. Wei, *RSC Adv.* **2017**, *7*, 46812.
[29] Y. G. Takei, T. Aoki, K. Sanui, N. Ogata, Y. Sakurai, T. Okano, *Macromolecules* **1994**, *27*, 6163.
[30] B. Jiang, H. Pang, *J. Polym. Sci. Part Polym. Chem.* **2016**, *54*, 992.
[31] T. Okano, N. Yamada, M. Okuhara, H. Sakai, Y. Sakurai, *Biomaterials* **1995**, *16*, 297.
[32] R. B. Grubbs, *Polym. Rev.* **2011**, *51*, 104.
[33] F. S. Bates, G. H. Fredrickson, *Phys. Today* **1999**, *52*, 32.

[34] C. Cummins, D. Borah, S. Rasappa, A. Chaudhari, T. Ghoshal, B. M. D. O'Driscoll, P. Carolan, N. Petkov, J. D. Holmes, M. A. Morris, *J. Mater. Chem. C* **2013**, *1*, 7941.
[35] Y. Mai, A. Eisenberg, *Chem. Soc. Rev.* **2012**, *41*, 5969.
[36] Y. Wang, X. Xu, P. Xu, X. Feng, Y. Zhang, F. Fu, X. Liu, *Polym. Int.* **2018**, *67*, 619.
[37] J. Böhmler, A. Ponche, K. Anselme, L. Ploux, *ACS Appl. Mater. Interfaces* **2013**, *5*, 10478.
[38] K. A. Savin, in *Writ. React. Mech. Org. Chem. Third Ed.* (Ed: K.A. Savin), Academic Press, Boston, **2014**, pp. 1–53.
[39] N. Maalouli, A. Barras, A. Siriwardena, M. Bouazaoui, R. Boukherroub, S. Szunerits, *Analyst* **2013**, *138*, 805.
[40] A. H. Soeriyadi, B. Gupta, P. J. Reece, J. J. Gooding, *Polym. Chem.* **2014**, *5*, 2333.
[41] X. Qiu, M. Ueda, H. Hu, Y. Sui, X. Zhang, L. Wang, *ACS Appl. Mater. Interfaces* **2017**, *9*, 33049.
[42] S. Won, D. J. Phillips, M. Walker, M. I. Gibson, *J. Mater. Chem. B* **2016**, *4*, 5673.
[43] M. Kaholek, W.-K. Lee, B. LaMattina, K. C. Caster, S. Zauscher, *Nano Lett.* **2004**, *4*, 373.
[44] H. G. Schild, *Prog. Polym. Sci.* **1992**, *17*, 163.

AUTHOR INFORMATION

Corresponding Authors

e-mail: herve.martinez@univ-pau.fr; laurent.billon@univ-pau.fr;

Funding Sources

ACKNOWLEDGMENT

We thank Dr. A. Khoukh and Dominique FOIX are acknowledged for fruitful discussions on NMR and XPS analysis. We thank F. Portail, C. Bessibes, and F. Casbas of Arkema Industry for the TEM analysis realized on propargyl-PEG4-thiol-capped gold nanoparticles, Francis Ehrenfeld and Anthony Laffore for constructing and making available a well-equipped instrument for angle contact analysis in a controlled environment.
